Int. J. Electrochem. Sci., 16 **(2021)** Article ID: 210324, doi: 10.20964/2021.03.47

International Journal of
ELECTROCHEMICAL
SCIENCE
www.electrochemsci.org

Preparation of Manganese Dioxide Nanozyme as Catalyst for Electrochemical Sensing of Hydrogen Peroxide

Na Zou[1,2,*], *Xianyong Wei*[1,3,*], *Zhimin Zong*[1], *Xin Li*[2], *Funa Meng*[2], *Zhaoxia Wang*[2]

[1] Key Laboratory of Coal Processing and Efficient Utilization, Ministry of Education, China University of Mining & Technology, Xuzhou 221116, Jiangsu, China
[2] Department of Chemistry and Chemical Engineering, Heze University, Heze 274015, Shandong, China
[3] State Key Laboratory of High-efficiency Coal Utilization and Green Chemical Engineering, Ningxia University, Yinchuan 750021, Ningxia, China
[*]E-mail: wei_xianyong@163.com (X. Wei), zgsdytzn@126.com (N. Zou)

Received: 5 November 2020 / *Accepted:* 30 December 2020 / *Published:* 31 January 2021

The two-dimensional manganese dioxide nanoflakes (MnO_2 NFs) with peroxidase-like activity was synthesized by a biomineralization method using bovine serum albumin (BSA) as a template. After then MnO_2 NFs was hybridized with reduced graphene oxide (rGO) for electrochemical sensing of hydrogen peroxide (H_2O_2). The composition and structure of MnO_2 NFs were characterized by Energy Dispersive X-ray Spectrometer (EDX) and Transmission Electron Microscope (TEM), and the morphology of hybridized material were characterized by Scanning Electron Microscopy (SEM). Electrochemical experiments showed that the hybridized material exhibited good sensing performance toward the reduction of H_2O_2 with broad linear ranges of 20 nM to 5 μM and 5μM to 800 μM. The limit of detection is 14.92 nM (S/N=3). The good sensing performance is ascribed to the synergistic effects of the special morphology of MnO_2 NFs and good conductivity of the reduced graphene oxide (rGO). The proposed sensor can be used for monitoring the H_2O_2 content in real biological environments with good stability, repeatability and selectivity.

Keywords: MnO_2 NFs, enzyme-like, H_2O_2 sensing, ultrasensitive

1. INTRODUCTION

Nanozyme is a kind of nanomaterials with enzymatic catalytic properties. Preparation of catalytically active nanomaterials has become an emerging field in biomimetic chemistry, which aimed at designing functional nanomaterials to mimic various intrinsic properties of natural enzymes [1, 2]. Nanozyme materials can be used as the substitutes of natural enzymes in the field of analytical sensing [3-6], environmental protection [7-9] and cancer treatment [10-13], because they are easier to be

prepared, more stable, and more widely used.

H_2O_2 is the most abundant active oxygen species in the body. Excessive H_2O_2 is considered to be a marker of oxidative stress, and it is associated with the occurrence and development of many diseases [14, 15]. In order to deeply understand the relationship of the oxidative stress with diseases, quantitative detection of H_2O_2 is necessary. The electrochemical sensor is one of the most suitable tools for detection of H_2O_2 in biological environments due to its intrinsic advantages, such as high sensitivity and selectivity, fast response, simplicity, low-cost and convenient operation. Many electrochemical H_2O_2 sensors have been designed to actualize the accurate and sensitive detection of H_2O_2. In these sensors, two main strategies were usually adopted, they are enzymatic catalysis (including natural enzymes and nanozymes materials) [16-18] and non-enzymatic nanomaterials catalysis [19-23]. Natural enzymes have high catalytic activity and substrate specificity, but they need expensive preparation and tedious purification, and they are easy to denature or degrade. Non-enzymatic nanomaterials have wider range of applications and more stable performance, but they suffered from the poor selectivity and sensitivity. Therefore, the use of nanozyme materials to construct H_2O_2 electrochemical sensors is a good selection.

In recent years, scientists have synthesized many kinds of peroxidase nanozyme materials by optimizing the synthesis conditions and changing the morphology and structure of the materials, and applied them to the colorimetric sensing of H_2O_2 [24-30]. For example, Kang and co-workers synthesized Mn_2O_3 hollow nanoparticles were by calcination and used them as a highly efficient sensing nanozyme for hydrogen peroxide and glucose [25]. Lei Huang et al synthesized VOx quantum dots using VO_2 as a precursor. The VOx quantum dots exhibit oxidase and peroxide-like activity and produce three different colors under three different concentrations of H_2O_2 [26]. Lei Han and colleagues [30] synthesized MnO_2 NFs and used them as a tandem nanozyme for the colorimetric detection of glucose and H_2O_2.

In this work, MnO_2 NFs nanozyme was synthesized using BSA as a biomineralization template [30-31] and then hybridized with rGO. The rGO is two-dimensional sheet with good physical and chemical properties, and it is easy to hybridize with MnO_2 NFs to form a stable dispersion. The hybridized material was used as a sensing platform to amplify the electrical signal and to decrease the reduction potential of H_2O_2. Based on this, the ultra-sensitive electrochemical detection of H_2O_2 molecules in biological environment was realized. Relative to colorimetric sensing, the use of substrates and large instruments is avoided, and it is more sensitive and more specific than non-enzymatic H_2O_2 sensing.

2. EXPERIMENTAL

2.1 Reagents and chemicals

Manganese acetate ($MnAc_2$) and BSA were purchased from Sigma Co. Ltd (USA), rGO powder was purchased from Nanjing XFNANO Materials Tech Co., Ltd (Nanjing, China), H_2O_2 (30%), sodium hydroxide (NaOH), ethyl alcohol, disodium hydrogen phosphate dodecahydrate

($Na_2HPO_4·12H_2O$) and monobasic sodium phosphate dihydrate ($NaH_2PO_4·2H_2O$) were purchased from Sinopharm Chemical Reagent Co. Ltd. (China). The phosphate buffer solution was prepared from 0.2 M NaH_2PO_4 solution and 0.2 M Na_2HPO_4 solution. Ultrapure water (18.2 MΩ cm^{-1}) was obtained from a Milli-Q ultrapure system (Qingdao, China). All reagents were of analytical grade and used without any further purification.

2.2 Synthesis of MnO_2 NFs nanozyme

MnO_2 NFs nanozyme was synthesized by chemical precipitation of $MnAc_2$ crystals in an alkaline solution containing BSA, the same with the method reported in the literature [11]. And the peroxidase-like activity of MnO_2 NFs had been strongly confirmed by colorimetric assay of H_2O_2 according to the paper. The specific steps are as follows: First of all, add 1 mg of BSA into a stirred solution of $MnAc_2$ (10 mL, 2×10^{-3} M), and keep stirring for 1 hour at room temperature. After BSA and Mn^{2+} were incubated for one hour, adjust the pH of the mixture solution to about 10 using NaOH solution (0.2 M) and H_3PO_4 solution (0.2 M). Keep stirring and 7 hours later, obvious nanoparticles were formed in the mixture solution. And then the obtained product was transferred to a centrifuge tube, and centrifuged at 5000 r/min for 5 min. After several times of washing and centrifugation, the obtained product is transferred out of the centrifuge tube and stored for future use.

2.3 Characterization

The morphology of materials was observed by SEM. Samples were prepared by drying a drop of aqueous solution of materials on a glass sheet and observed by SEM SU8010 (Hitachi, Japan). The composition and structure of materials were characterized by TEM (Tecnai G2 F20, FEI, USA, operation voltage 120 kV). A combined energy-dispersive X-ray spectroscopy and elements mapping analysis system attached to the TEM were used for elemental analysis.

All electrochemical measurements were performed at room temperature on a CHI 920C electrochemical workstation. Electrochemical experiments were conducted with a three-electrode unit structure. The modified GCE was used as the working electrode, the saturated calomel electrode was used as the reference electrode, and platinum wire was used as the counter electrode. The 0.2 M phosphate buffer purified by N_2 was used as the electrolyte for H_2O_2 sensing.

2.4 Construction of the sensor and H_2O_2 Sensing

The experiment steps of construction of the sensor and H_2O_2 Sensing are as followed: Firstly, the glassy carbon electrode (GCE) (diameter 3 mm) is polished on the suede board with Al_2O_3 (0.03 μ m) powder until it is a mirror surface. And then monitor it by cyclic voltammetry in 5 mM $[Fe(CN)_6]^{3-/4-}$ solution. The voltammetric characteristic curve of GCE is observed, and the negative and positive peaks of the voltammetric characteristic curve are obtained. If $\Delta E_p < 0.08$ V, the surface of GCE has been well activated. Rinse the activated GCE with ultra-pure water to make sure the electrode surface

is clean, and dried naturally at room temperature. The prepared rGO solution should be ultra-sonicated for 10 minutes before use, in order to destroy the agglomeration of nanomaterials, and ensure the uniform dispersion of the modified solution. After the surface of GCE is completely dry, 5 μL of rGO mixture is casted to the surface of GCE by using a pipette gun, and then it is dried again at room temperature. The modified electrode is recorded as rGO/GCE. Then the prepared MnO_2 NFs were covered on the rGO/GCE and recorded as MnO_2 NFs/rGO/GCE. After that, it is stored in cold for further use. The modified electrode is used as the working electrode in the next experiment.

3. RESULTS AND DISCUSSION

3.1 Characterization of MnO_2 NFs

From the analysis on the EDX spectrum (Figure 1a), it was found that manganese and oxygen are present in the spectrum, which means MnO_2 was obtained by chemical precipitation under basic conditions. The appearance of copper and carbon is due to the use of ultra-thin carbon film copper mesh substrate. The EDX result is consistent with a literature reports which synthesized MnO_2 nanoparticles under acidic conditions [32].

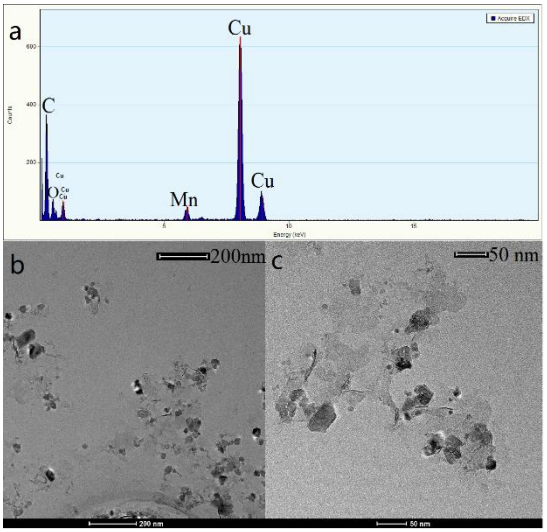

Figure 1. The morphology and composition of MnO_2 NFs. (a) TEM-EDX pattern spectra of MnO2 NFs. (b, c) TEM images of MnO_2 NFs with different magnifications.

In order to investigate the nanostructure of MnO_2, TEM was measured with different magnification (Figure 1b, 1c). Most of the morphology is two-dimensional thin thickness，and the material is recorded as MnO_2 NFs. It is proved that we have successfully synthesized flaky MnO_2 nanomaterials under the given experimental conditions using biomineralization methods. The obtained material was then modified on GCE with rGO, and the surface morphology of the deposited material was scanned using SEM (Figure 2). It is found that the size of the material is about 100 nm, and the morphology of the material is sheet stacked. Compared with other literatures, the MnO2 NFs

synthesized in this paper has a two-dimensional nanometer morphology, it is different from flower-like or sphere MnO_2 which was synthesized by one step acidification [32, 33].

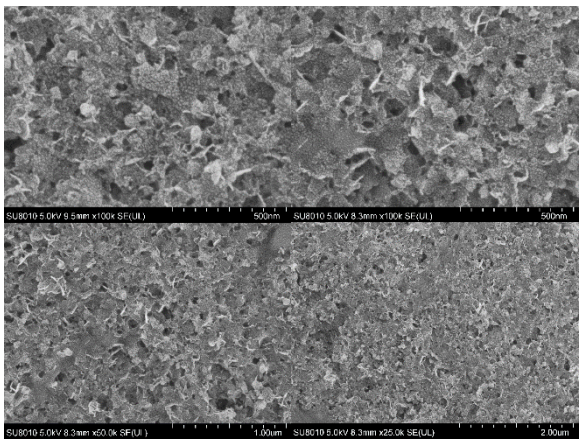

Figure 2. SEM images of MnO2 NFs/rGO/GCE with different magnifications.

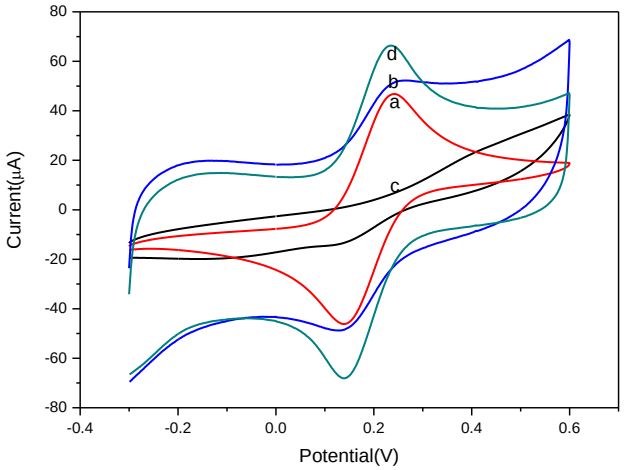

Figure 3. Cyclic Voltammograms obtained in 1 mM $[Fe(CN)_6]^{3-/4-}$ solution containing 0.1 M KCl at bare GCE (curve a), rGO/GCE (curve b), MnO_2 NFs/ GCE (curve c) and MnO_2 NFs/rGO/GCE (curve d).

3.2 Electrochemical behavior of different modified electrodes

In the constructing process the sensor, the electrochemical behavior of GCE was studied by cyclic voltammetry (CV). The CV scan was carried out in a 1 mM $[Fe(CN)_6]^{3-/4-}$ solution containing 0.1 M KCl. The current response of the modified electrode to $[Fe(CN)_6]^{3-/4-}$ can reflect the status of modified electrode. Many literatures have used this method to characterize the electron transfer of the electrode. Similar to some literatures [21-23], this experiment also obtained similar expected results. As shown in figure 3, a couple of expectedly reversible redox peaks were obtained on the GCE. After a

layer of rGO was modified on bare GCE, the redox peak potentials were almost unchanged, and the peak current is increased significantly, indicating that the rGO provided large specific surface area and excellent electrical conductivity for electron transfer. However, on the MnO_2 NFs/GCE, $[Fe(CN)_6]^{3-/4-}$ showed irreversible electrochemical behavior and no obvious redox peaks were obtained. The results showed that the MnO_2 NFs is not a good electrode surface modifier for improving the conductivity of electrode. Therefore, it is necessary to hybridize it with rGO to compensate the shortcoming of its poor conductivity. As we expected, on the MnO_2 NFs/rGO/GCE electrode, a large peak current response was obtained.

The excellent electrochemical properties of the MnO_2 NFs/rGO nanocomposites for electrochemical response of H_2O_2 were showed by for recording the CV of different modified electrodes in pH 7.4 PBS solution containing 20 mM H_2O_2 with a scanning rate of 0.08 V s^{-1} (Figure 4). It was found that, on the bare GCE, rGO/GCE, MnO_2 NFs/GCE and MnO_2 NFs/rGO/GCE, no obvious current response was obtained in pH 7.4 PBS solution without of H_2O_2. As we add H_2O_2 in the pH 7.4 PBS solution, the current increased significantly as the sequence of bare GCE, rGO/GCE, MnO_2 NFs/GCE and MnO_2 NFs/rGO/GCE, indicating that H_2O_2 had no obvious electrochemical response on the bare GCE and the MnO_2 NFs have excellent electrocatalytic activity for the reduction of H_2O_2. After the MnO_2 NFs hybridized with rGO, the biggest electrochemical response of H_2O_2 was obtained on the MnO_2 NFs/rGO/GCE, indicating that they played synergistic effect for the H_2O_2 sensing. The rGO can increase the electrical conductivity and also prevent the aggregation of the MnO_2 NFs, thus providing more electrical sites for the H_2O_2 reaction.

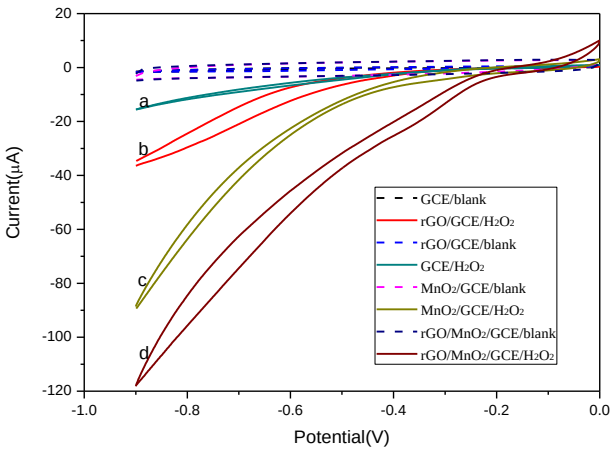

Figure 4. Cyclic Voltammograms obtained in 0.1 M pH 7.4 PBS solution at bare GCE (curve a), rGO/GCE (curve b), MnO_2 NFs/ GCE (curve c) and MnO_2 NFs/rGO/GCE (curve d) with (solid line) and without (dash line) 1 mM H_2O_2.

3.3 Working curve and linear relationship

In order to further verify the electrochemical sensing properties of the sensor, the redox properties of different concentrations of H_2O_2 to MnO_2 NFs/rGO were investigated, and the optimal

potential for detecting H_2O_2 were found. As shown in figure 5, the CV curve showed a regular change after adding equal amounts of H_2O_2 (5-1000 μ M). Obviously, the cathode current of the MnO_2 NFs/rGO sensor increases with H_2O_2 concentration increasing between -0.8 V and -0.3 V relative to the saturated calomel electrode.

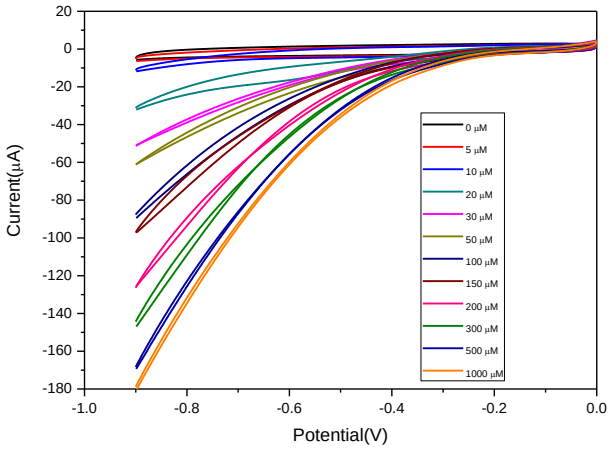

Figure 5. Cyclic Voltammograms obtained in 0.1 M pH 7.4 PBS solution at MnO_2 NFs/rGO/GCE sensor with different concentration of H_2O_2 from 0-1000 μM.

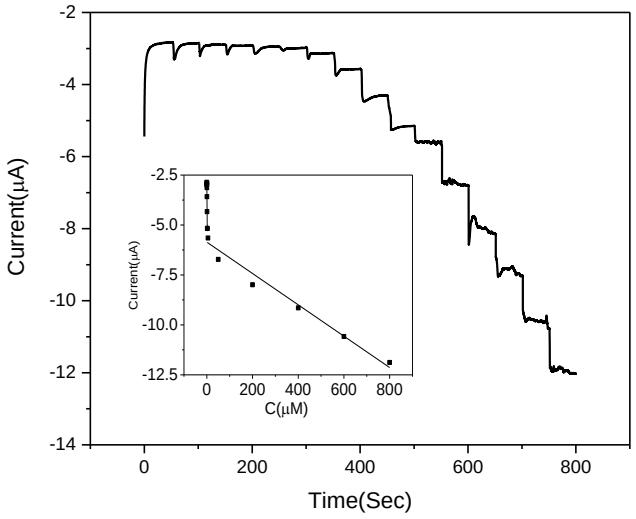

Figure 6. Amperometric i-t curve of H_2O_2 at MnO_2 NFs/rGO/GCE sensor at different concentrations from 20 nM to 800 μM by continuous addition of H_2O_2 in 0.1 M PBS (pH 7.4). Inset: plot of current, i vs. H_2O_2 concentration.

The effectiveness of MnO_2 NFs/rGO nanoparticles modified eletrode for H_2O_2 sensing was demonstrated in the next experiment, by the means of typical steady-state current response of synthetic materials. The effect of operating potential on the ampere response of MnO_2 NFs/rGO/GCE to 0.5 mM H_2O_2 was investigated firstly. H_2O_2 exhibits a stable current response at MnO_2 NFs/rGO/GCE at different potentials, indicating that all potentials can be used for amperometric measurements.

However, the interference effect of dissolved oxygen will be significant at the polarization potential. Therefore, -0.3 V is suitable for further measurements.

Electrocatalytic reduction of H_2O_2 current detection is an important detection method in electrochemical analysis, and the generated current is proportional to the concentration of the species produced. Figure 6 shows a typical amperometric response of MnO_2 NFs/rGO/GCE to -0.3 V for continuous addition of H_2O_2 in 0.1 M PBS (pH 7.4). It can be clearly seen from the figure that when H_2O_2 is added, the current response current increases and reaches a steady state within a few seconds. It shows that the MnO_2 NFs/rGO/GCE electrode has good electrocatalytic performance. The MnO_2 NFs/rGO/GCE electrode current response was linear with H_2O_2 concentrations ranging from 20 nM to 5 μM and 5 μM to 800 μM with correlation coefficients of 0.983 and 0.969, respectively. In the range of 20 nM to 5 μM, the linear regression equation I_p (μA) = -2.886 + (-1.2095) ·C (μM) is obtained, and in the range of 5 μM to 800 μM, the linear regression equation is I_p (μA) = -5.857 + (-0.0079) ·C (μM). The detection limit is 14.92 nM (S/N = 3). The outstanding value of this nanozyme H_2O_2 sensor lies in its ultra-low detection linearity range compared with other sensors (Table 1). The improvement in H_2O_2 detection performance of MnO_2 NFs/rGO/GCE can be attributed to the increasing conductivity by adding rGO and good nano-enzyme activity of MnO_2.

Table 1. A comparison of proposed method of sensing H_20_2 with previous electrochemical studies.

Material/electrode	Linearity Range (μ M)	LOD (μ M)	Ref.
Au–MnO_2–rGO nanocomposite	0.1–22 and 22–12600	0.05	34
flower-like MnO_2	80-12780	20	35
f-MWCNTs/MnO_2	5-4530	0.952	36
Mn_2CuO_4	0.036 -9300	0.013	37
Co_3Mn-LDH	110-1200	86	38
$COF_{ETTA-TPAL}$-Fc$(COOH)_2$	1.1–500	0.009	39
rGO/MnO_2 nanozyme	0.02-5 and 5-800	0.015	This work

3.4 Repeatability, stability and selectivity

In order to evaluate the repeatability of the prepared sensor, the relative standard deviation (RSD) of the sensor for determination of 5 mM H_2O_2 was calculated for 5 consecutive experiments in pH 7.4 phosphate buffer and RSD <3.84% (n = 4). This indicates that the modified electrode has good repeatability. Five electrodes were prepared using the same preparation process to evaluate the reproducibility of the sensor. The RSD current was 3.5% for 5 mM H_2O_2, showing acceptable reproducibility. The storage stability of the method is further studied. The MnO_2 NFs/rGO/GCE was stored at 4 ℃ and the current response was tested to maintain about 93.6% of the original signal over 30 days, indicating significant long-term stability. The anti-interference ability of the electrodes was demonstrated by amperometric method using L-cystine (L-cys), uric acid (UA) and ascorbic acid (AA). As expected, MnO_2 NFs/rGO modified GCE exhibited a low response when each interfering substance was continuously added, but a significant current was observed when 0.04 mM H_2O_2 was added. These results indicate that the sensor has a unique selectivity for H_2O_2.

3.5 Real sample detection

The practicality of the developed sensor in the actual sample was verified by detecting H_2O_2 in the urine (as real samples) using standard addition method under the optimal conditions. The urine was diluted with 0.1 M PBS (pH 7.4). The calibration curve was used to calculate the content of H_2O_2 in the sample, and the recovery was between 98.66 and 101.48 %. The RSD was below 4.17% (n = 3).

4. CONCLUSIONS

The two-dimensional enzyme-like material MnO_2 NFs was synthesized by biomineralization method, and rGO was hybridized to improve the electron conduction performance of the electrode surface. Based on the hybridized material, a sensitive electrochemical sensor for H_2O_2 was constructed. The sensor can directly and rapidly read the content of H_2O_2 in a wide concentration range, and can be used in environmental monitoring and biological analysis. It is not only suitable for the detection of trace H_2O_2 concentration in vivo and in vitro in biological environment, but also suitable for monitoring the inhibited enzymatic reaction when H_2O_2 concentration is too high. In addition, the enzyme-like activity of MnO_2 NFs will be important for the design of enzymatic systems and for further potential application in anti-inflammatory, anti-tumor and maintenance of metabolic balance.

ACKNOWLEDGEMENTS
This work was financially supported by the National Natural Science Foundation of China (Grants 21776298 and 21576280), the National Key Research and Development Program of China (Grant 2018YFB06046002), the Natural Science Foundation of Shandong Province, China (ZR2020QB090).

References

1. Y. Huang, J. Ren, X. Qu, *Chemical Reviews*, 119 (2019) 4357.
2. H. Dong, Y. Fan, W. Zhang, *Bioconjugate Chemistry*, 30 (2019) 1273.
3. B. Jiang, D. Duan, L. Gao, *Nat. Protoc.*, 13 (2018) 1506.
4. A. Othman, A. Hayat, Andreescu S, *ACS Applied Nano Materials*, 1 (2018) 5722.
5. H. Liu, Y. N. Ding, B. Yang, *ACS Sustainable Chemistry & Engineering*, 6 (2018) 14383.
6. P. Wang, L. Cao, Y. Chen, *ACS Applied Nano Materials*, 2 (2019) 2204.
7. E. N. Efremenko, I. V. Lyagin, N. L. Klyachko, T. Bronich, N. V. Zavyalova, Y. H. Jiang, A. V. Kabanov, *Controlled Release*, 247 (2017) 175.
8. H. B. Li, L. Ma, L. Y. Zhou, J. Gao, Z. H. Huang, Y. He, Y. J. Jiang, *Chem. Commun.* , 54 (2018) 10754.
9. Z. Sui, Y. Zhang, T. Wang, *Energy & Fuels*, 32 (2018) 6584.
10. L. Fan, X. Xu, C. Zhu, *ACS Applied Materials & Interfaces*, 10 (2018) 4502.
11. J. Li, J. Huang, Y. Lyu, *Journal of the American Chemical Society*, 141 (2019) 4073.
12. P. Zhu, Y. Chen, J. Shi, *ACS Nano*, 12 (2018) 3780.
13. D. P. Cormode, L. Z. Gao, H. Koo, *Trends Biotechnol*, 36 (2018) 15.
14. K. Dhara, D. R. Mahapatra, *Journal of Materials Science*, 54 (2019) 12319.

15. Y. Su, X. Zhou, Y. Long, W. Li, *Microchimica Acta*, 185 (2018) 114.
16. R. Zhang, C. Jiang, X. Fan, R. Yang, Y. Sun, C. Zhang, *Microchimica Acta*, 185 (2018) 58.
17. X. Wu, H. Zhang, K. Huang, *Bioelectrochemistry*, 120 (2018) 150.
18. S. Rinky, V. Nandimalla, B. Sushmee, *Microchimica Acta*, 185 (2018) 399.
19. T. G. Choleva, V. A. Gatselou, G. Z. Tsogas, D. L. Giokas, *Microchimica Acta*, 185 (2018) 22.
20. M. Asif, A. Aziz, A. Q. Dao, A. Hakeem, H. Wang, S. Dong, G. Zhang, F. Xiao, H. Liu, *Analytica Chimica Acta*, 898 (2015) 34.
21. S. He, B. Zhang, M. Liu, *RSC Advance*, 4 (2014) 49315.
22. Z. Li, Y. Jiang, Z. Wang, W. Wang, Y. Yuan, X. Wu, X. Liu, M. Li, S. Dilpazir, G. Zhang, D. Wang, C. Liu, J. Jiang, *Microchimica Acta*, 185 (2018) 501.
23. J. Ge, K. Xing, X. Geng, Y. Hu, X. Shen, L. Zhang, Z. Li, *Microchimica Act*a, 185 (2018) 559.
24. G. Vinothkumar, I. L. K. S. Arun, Babu, *Inorg Chem*, 1 (2019) 349.
25. C. Chen, D. Xiong, M. Gu, C. Lu, F.Yi, X. Ma, *ACS Applied Materials Interfaces* 12 (2020) 35365.
26. L. Ding, S. Chen, W. Zhang, *Analytical Chemistry*, 12 (2018) 7544.
27. Z. Kang, R. K. Kankala, B. Chen, C. Fu, S. Wang, A. Chen, *ACS Applied Materials & Interfaces*, 11 (2019) 28781.
28. Huang, Y. Niu, R. Li, *Analytical Chemistry*, 21 (2019) 5753.
29. Han, H. Zhang, D. Chen, *Advanced Functional Materials*, 28 (2018) 180018.
30. G. Junli, Y. Lingling, X. Huijie, Z. Chenxi, D. Zhenqing, G. Zhida, S. Yanyan, *Analytical Chemistry*, 91 (2019) 13746.
31. M. Mohammad, A. Razmjou, K. Liang, M. Asadnia, V. Chen, *ACS Applied Materials Interfaces*, 11 (2019) 1807.
32. K. Kohila Rani, R. Devasenathipathy, S. Wang, C. Yang, *Ionics* 23(2017) 3219.
33. W. Bai, X. Zhang, S. Zhang, Q. Sheng, J. Zheng, *Sensors and Actuators B: Chemical*, 242 (2017) 718.
34. L. Wang, M. Deng, G. Ding, S. Chen, F. Xu, *Electrochimica Ac*ta, 114 (2013) 416.
35. W. Bai, X. Zhang, S. Zhang, Q. Sheng, J. Zheng, *Sensors and Actuators B*, 242 (2017) 718.
36. K. Rani, R. Devasenathipathy, S. Wang, C. Yang, *Ionics*, 23 (2017) 3219.
37. P. Balasubramanian, M. Annalakshmi, S. Chen, T. Sathesh, T. Peng, T. Balamurugan, *ACS Appl. Mater. Interfaces*, 10 (2018) 43543.
38. H. Farhat, C. Taviot-Gueho, G. Monier, V. Briois, C. Forano, C. Mousty *J. Phys. Chem. C*, 124 (2020) 15585.
39. H. Liang, M. Xu, Y. Zhu, L. Wang, Y. Xie, Y. Song, L. Wang, *ACS Appl. Nano Mater.* , 3 (2020) 555.